Formation of Fiberwebs from Staple Fibers with Controlled Fiber Orientation Using Electrostatic Forces: Theoretical Analysis

Yiyun Cai, Ph.D. [1], Abdelfattah Mohamed Seyam, Ph.D. [1], Yong K. Kim, Ph.D. [1]

[1]North Carolina State University, Raleigh, North Carolina USA

Correspondence to:
Dr. Abdelfattah Mohamed Seyam, Ph.D. email: aseyam@tx.ncsu.edu

ABSTRACT

Current web formation technologies used by the nonwovens industry do not provide positive control over fiber orientation and it is difficult to generate lightweight webs from staple fibers with these processes. The aim of this research is to develop new methods of fiberweb formation using electrostatic force, where orientation and orientation distribution of staple fibers are positively controlled. We carried out theoretical analysis and constructed computer models for this approach. Our analysis considered the effects of geometric configurations of fiber feeding and web formation zone, electrostatic and airflow field parameters, and the fiber's initial conditions at the feeding zone on fiber orientation. The theoretical analyses and computer modeling of the electrostatic web forming process provide better insights into this method and serve as a powerful tool for engineering development. Numerical results were obtained and presented for a range of processing variables.

INTRODUCTION

The main technologies that are currently used in the nonwovens industry to form fiberwebs from staple fibers are carding, carding and cross-lapping, air lay, and wet lay. These methods do not provide positive control over fiber orientation and fiber orientation distribution (FOD). In these methods, different trials with different processing parameters are conducted, and the FOD is measured for each trial either directly or through the analysis of fiberweb and/or fabric properties. This is a lengthy procedure that is often repeated until some acceptable FOD and fabric properties are achieved within the limitations and variability of the fiberweb forming system. The lack of positively controlling fiberwebs' FOD leads to nonwoven fabrics with significant difference between the strengths in the cross- and machine-directions and the inconsistency in obtaining nonwoven fabric with desired properties. In addition, the non-uniformity in fiberweb basis weight produced by these traditional methods also limits their capability of making lightweight fiberwebs. This is due to the inherent difficulties in positive FOD control.

Our research addresses the development of a new technology for producing fiberwebs from staple fibers with positively controlled fiber orientation and FOD by the use of electrostatic forces acting on charged fibers. This innovative approach will also improve the industry's ability of producing lightweight structured fiberwebs with engineered properties.

Earlier efforts in fiber transfer, orientation and separation in electrostatic field include the review and analysis in electrostatic yarn spinning by Dogu [1,2], as well as Robert Jr. *et al* 's research on an improved electrostatic yarn spinning system equipped with a twisting and fiber feeding device [3]. In these electrostatic yarn spinning systems, corona-charging methods were employed to impart static charge in fibers. These systems experienced difficulties in controlling fiber orientation and speed, possibly due to the fact that the corona charge was not reliable and charges imparted on the fibers were varying. Yao invented an apparatus for electrostatic opening and short fiber separation. This device aligned cotton fibers in a carded web using electrostatic field forces acted upon fibers by a pair of metal belts, which were connected to high DC voltage [4]. In addition to yarn manufacturing applications, electrostatic field has been extensively utilized in electrospinning of nanofibers and microfibers [5, 6]. The alignment of electrospun nanofibers was experimentally addressed by numerous researchers. An example of this work is published by Theron et al [7].

In Nagi-Zade and Grosberg's research on fiber orientation in electrostatic fields, they reported that fibers with only field-induced polarization did not have enough force available to straighten such fibers [8]. In a recent work, Hou studied short fiber motion in electrostatic fields by high-speed digital

photography [9]. It was found that short fibers with a conductive surface finish were oriented perpendicular to the equi-potential lines and moved along the field lines in an electrostatic field. To achieve this orientation, it is essential that the fibers have a uniform conductive surface finish that is capable of imparting a surface resistivity of 10^5– 10^7 Ω/Square for direct charging.

It is evident that proper arrangement of electrodes, direct charging and a conductive surface finish are needed to provide the positive control of fiber orientation in a fiberweb with minimum or no "fiber hook" formation. Required time to charge fibers in an electrostatic field are strongly correlated to the field strength. For example, a cotton fiber resting on a positive pole acquires a charge amount in the range of $2x10^{-11}$ - 4 x 10^{-11} C in 0.023 second and moves toward the negative pole at an average speed of 7.1 m/sec [8]. Charge transferred from the electrode to polyester and other synthetic fibers is lower than the amount acquired by cotton fibers. In this research, conductive surface finish and direct charging are employed for positively controlling the fiber motion that allows for the control of FOD, and therefore the fiberweb basis weight and its uniformity.

However, the precise control of fiber orientation and motion with electrostatic forces to form fiberwebs with predetermined FOD has significant challenges. The problems stem from non-uniformity in conductive surface finish applied on each fiber, fiber geometrical parameters, and deviation of the electrostatic field lines from the theoretically predicted one and other variations.

In order to provide better understanding for achieving the goal of positive control over fiber orientation and FOD, we conducted theoretical analysis and computer modeling of fiber movement and orientation in an electrostatic field. These analyses and modeling of the processing variables also serve as a tool for developing and optimizing prototypes of electrostatic fiberweb forming systems.

We analyzed the forces acted on a fiber in an electrostatic field and constructed mathematical models by integrating the governing equations with a model that describes the fiber configuration. The model considered different electrostatic field strengths and airflow fields. The geometrical configurations of a computational region (the region in which fiber movement and web formation take place) were deduced. The computational region configuration is the determining factor in designing and engineering the real equipment. A numerical method was developed for solving the model. For result analysis, visualization programs were established to illustrate and animate the simulated fiber movements. Fiber delivery and orientation with different conditions were analyzed using the computer modeling results.

CONCEPT DEVELOPMENT OF A SYSTEM FOR ORIENTING FIBERS USING ELECTROSTATIC FORCE

Figure 1 shows the concept of a device that produces fiberweb with positively controlled FOD by using electrostatic force. In order to control fiber orientation in a specified direction, an electrostatic field with parallel field lines is needed. The field lines should be in the same direction of the desired fiber orientation. This can be achieved by arranging two flat conductive surfaces as electrodes opposing to each other. One electrode is grounded (electrode *A* in *Figure 1a*) and the other one is charged with high voltage (electrode *B* in *Figure 1a*). The space between these two electrodes forms the fiber-orienting zone. Fibers are charged with the same sign as electrode *B*. An aspirator and feed rollers dispense the fibers into the electrostatic field. The aspirator is connected to high voltage for charging the fibers. On the bottom of the fiber orienting zone is the fiber collection surface. One design of this surface is a moving vacuum belt, which causes the oriented fibers to adhere to the collecting surface and transport the produced web to the next step. In the "Results and Discussion" section, for the purpose of revealing the fiber's moving status such as orientation and speed in the entire electrostatic field, all our modeling results show fiber trajectories from electrode B to A. But in fact, with properly controlled parameters such as H2, the fiber will contact the vacuum belt and be transported to a take up roller before it hit electrode A (*Figure 1*).

One of our computer models is based on the above concept. The computer model can predict the fiber movements and trajectory in the airflow and electrostatic fields. The computational region of the model is depicted in *Figure 1a* based on the geometrical configuration of our concept. H1 is the height of the electrodes, and H2 is the height at which the fiber is discharged from aspirator. Right-hand Cartesian coordinates are adopted here, where the *x*-direction is the machine direction (MD), the *z*-direction is cross machine direction (CD), the *y*-direction is perpendicular to the *x*-*z* plane, and the origin is located at the center of the bottom of the grounded electrode (the left electrode in *Figure 1a*).

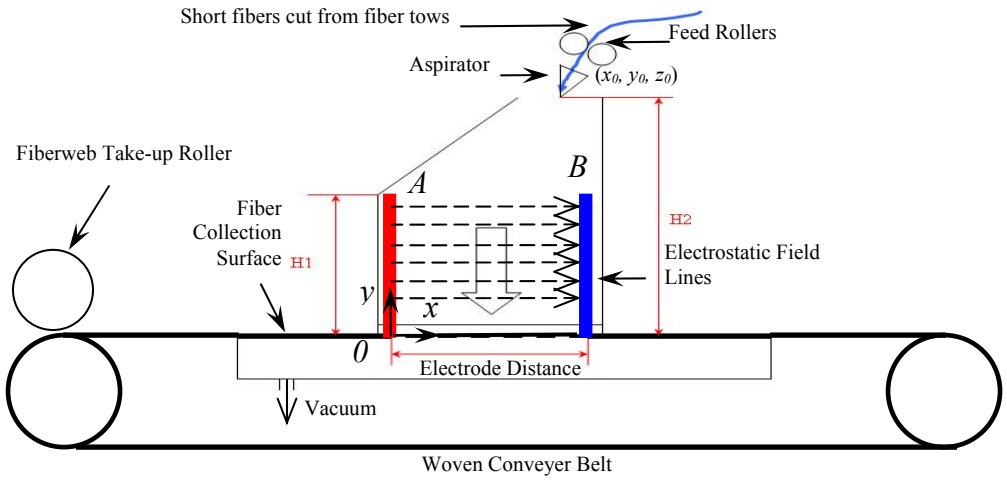

(a)

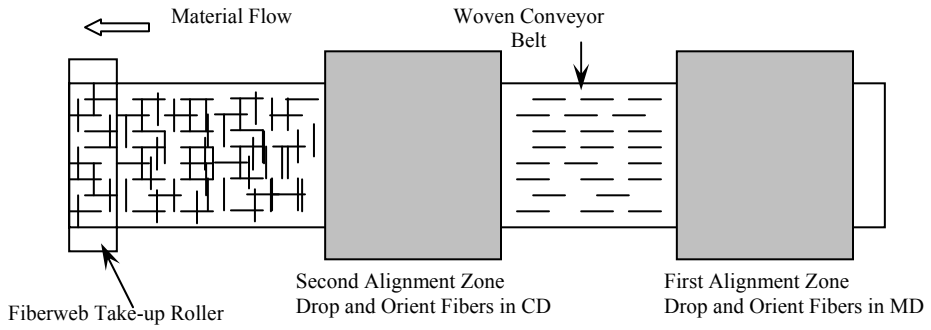

(b)

Figure 1. System concept and computational region

Fibers are dispensed from the aspirator at position (x_0, y_0, z_0).

The concept and model discussed above control fiber orientation in one direction; other directions can be achieved by introducing multiple pairs of electrodes and aspirators along the same fiberweb production line and properly arranging the electrostatic field lines between each pair of electrodes. *Figure 1b* is the top view of two fiber orienting zones that make the fiberweb, with orthogonally distributed fibers from a MD and a CD laydown. Vacuum under the porous woven belt is used to keep the fiber orientation undisturbed. Combination of vacuum and adhesive layer is also possible to maintain the fiber orientation and the fiberweb integrity.

ANALYSIS OF FORCES ACTING ON A FIBER IN AN ELECTROSTATIC FIELD

Figure 2 represents one element *ds* of a moving fiber of length *L* in an electrostatic field. The basic governing equation of this element can be written as

$$\rho_l \frac{\partial \vec{v}}{\partial t} = -\frac{\partial \vec{F}_s}{\partial s} + \vec{f}_{surf} + \vec{f}_{body} \qquad (1)$$

where ρ_l is fiber linear density; $\vec{v}$ is element velocity; $\vec{F}_s$ is concentrated force; $\vec{f}_{surf}$ is surface force of unit length, which only acts on the fiber's surface; $\vec{f}_{body}$ is body force of unit length, which acts on the entire fiber's volume. In computer simulations, the concentrated forces $\vec{F}_s$ and $\vec{F}_{s+ds}$ (*Figure 2a*) acting on this element are considered as interactions from elements that connected to it; surface force $\vec{f}_{surf}$ is air drag; body force $\vec{f}_{body}$ is a combination of the fiber's gravity, electrostatic force, and buoyancy.

The selection of an applicable description of the fiber configurations is the key that links the above discussed governing equations to computer simulations, in which fibers are studied in discrete

forms. In this research, the configurations and characteristics of a fiber are described (assumed) as a series of spheres connected by inflexible zero-diameter, zero-mass rods, which are depicted in *Figure 2b*. Under these assumptions, the air drag on each fiber section can be easily computed in such a way that air flow passes the spheres at each section's ends.

The fiber is considered to be inextensible. Therefore, the following dynamic equation can be used to describe the movement of an element that consists of one single sphere and a connecting rod of zero-mass and zero-diameter of the fiber in the electrostatic field

$$m\vec{a}_i = \vec{f}_{i-1,i} + \vec{f}_{i+1,i} + \vec{f}_a + \vec{f}_b + \vec{f}_g + \vec{f}_e \qquad (2)$$

where m is mass of a single sphere; $\vec{a}_i$ is acceleration of the sphere; $\vec{f}_a$ is air drag; $\vec{f}_b$ is buoyancy; $\vec{f}_g$ is gravity; $\vec{f}_e$ is electrostatic force; $\vec{f}_{i-1,i}$ is action from sphere *i-1* to *i;* $\vec{f}_{i,i+1}$ is action from sphere *i* to *i+1*.

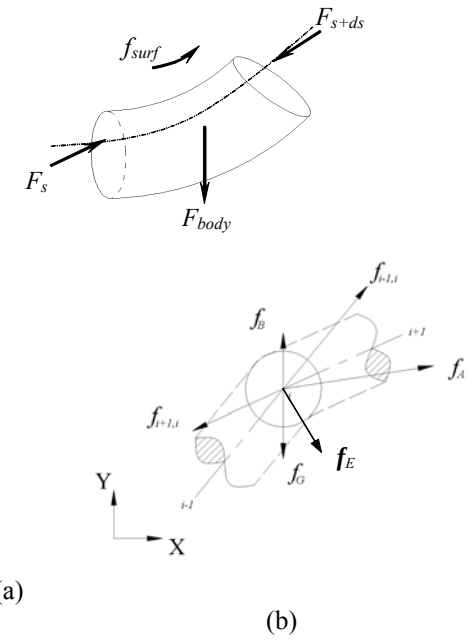

(a) (b)

Figure 2a. Forces acting on a fiber element, (b): Forces acting on one sphere

The electrostatic force and air drag on the fiber then can be computed from equations 2 and 4.

The electrostatic force f_e experienced by each section is

$$\vec{f}_e = \vec{E}q_i \qquad (3)$$

Where E is the electrostatic field strength, and q_i is the static charge on the i^{th} sphere. Based on Nagi-Zade and Grosberg's research [5], the polarization of a fiber's surface charge is approximately linearly distributed along the fiber's length. Then for each discrete fiber section, electrostatic charge is calculated in such a way that the summation of every section's surface charge equals to the fiber's net charge Q, and each section's charge is linearly polarized against the direction of the field lines.

Calculation of the air drag is decided by the element's Reynolds number: $\mathrm{Re} = U_\infty D/\tau$. Where D is the diameter of a sphere, U_∞ is difference between the velocity of an element and its incoming airflow speed, and τ is the kinetic viscosity of air. Air drag F_a can be calculated from following equation:

$$F_a = C_D \pi r_0^2 \left(\frac{1}{2}\rho U_\infty^2\right) \qquad (4)$$

where r_0 is the radius of the sphere and C_D is air drag coefficient. If the Reynolds number is smaller than five, the air drag coefficient is calculated by Oseen's Equation, which is:

$$C_D = \frac{24}{\mathrm{Re}}\left(1 + \frac{3}{16}\mathrm{Re}\right) \qquad (5)$$

When the Reynolds number is larger than five, the air drag coefficient is calculated by interpolated experimental data [10].

COMPUTER MODELING

Numerical algorithms were developed in solving the derived set of equations. These equations form the basis to predict the movement of the fiber at a particular instance of time and its trajectory.

In order to solve Equations 1-4, one objective function F_{OBJ} should be selected for the computational model. It is defined as:

$$F_{OBJ} = \sum_{i=1}^{K} (L_i^{(n+1)} - 1)^2 < \varepsilon \qquad (6)$$

This function is selected because during the entire fiber movement, the extension of a fiber is neglected and so the length of every single segment (L_i in

Equation 6) is considered constant, and therefore $\sum_{i=1}^{K} L_i$ should equal to the fiber length. ε is a predetermined convergence criterion. The search direction for this convergence criterion is

$$-[\frac{\partial F_{OBJ}}{\partial f_{0,1}}, \frac{\partial F_{OBJ}}{\partial f_{1,2}}, \cdots, \frac{\partial F_{OBJ}}{\partial f_{i-1,i}}]^T \qquad (7)$$

For simplicity, we introduced the following dimensionless length, speed and force parameters in the model:

Dimensionless Length: $X = x(\frac{1}{L})$, $Y = y(\frac{1}{L})$, $Z = z(\frac{1}{L})$

Dimensionless Speed: $V = v(\frac{\Delta t}{L})$

Dimensionless Force: $F = f(\frac{\Delta t^2}{mL})$ (8)

Initial conditions include fiber initial speed, incident angle, and position. Fiber length, diameter, and density, airflow speed, and electrostatic field strength are employed in the computation as constants. Geometrical parameters of the computational region, electrode distance and heights, are used to specify boundary conditions. Equations 6 and 7 are integrated with the basic governing equations to generate the discrete form equations that are used in the computer code. Computation codes were written in C++. The solutions are robust during computations. The solutions contain the velocities and space coordinates of all segments of the modeled fiber at each specific time during the movement.

Visualization programs were developed for displaying and analyzing the data from solutions. The program displays every single position of the fiber and its trajectory in the modeled space at any instance of time. They were developed using the C++ with OpenGL. They are also capable of generating animations of the fiber movements. The snapshots of fiber movements in the following section were generated by the visualization program.

RESULTS AND DISCUSSIONS

Fibers in the model were simulated as 0.02 m long staple fibers. The parameters of three types of fiber (rayon, polyester and nylon) are listed in *Table I*. The simulated fibers were considered to be negatively charged at 4.0 X 10^{-11} C. This charge was imparted by contacting the high negative potential with the aspirator surface.

Table I. Fiber Properties

Fiber Type	Rayon	Polyester	Nylon
Fiber Density:	1.55×10^3 kg/m^3	1.37×10^3 kg/m^3	1.10×10^3 kg/m^3
Fiber Diameter:	1.5×10^{-5} m	1.5, 4.5×10^{-5} m	1.5×10^{-5} m
Fiber Length:	2.0×10^{-2} m	2.0×10^{-2} m	2.0×10^{-2} m

Results were used to carry out studies on the optimization of the system's geometrical and operational parameters. The above three different fibers' behaviors in the electrostatic field were investigated. Resultant data was analyzed and displayed by the visualization program, which are shown in the following snapshots (*Figures 3 and 4*).

Optimization of the Electrodes' Height

Initially, the height of the positive electrode (H1 in *Figure 1*) proposed for a prototype was 0.5 m. The consideration was that if the electrodes were not high enough, the alignment of fibers cannot be assured because the fiber could hit the bottom before it was aligned.

Computer modeling results show with a field strength of 250 KV/m, a speed of a fiber entering the orienting zone at 25 m/s, and an incident angle of 20 degrees, the rayon fiber can be aligned to the direction of the field lines after movement in the *y*-direction a distance of 0.08 m (*Figure 3*). It is obvious that a 0.5 m electrodes height is more than sufficient to provide a fiber orienting zone under these conditions. Therefore compact design can be achieved by utilizing computer modeling results.

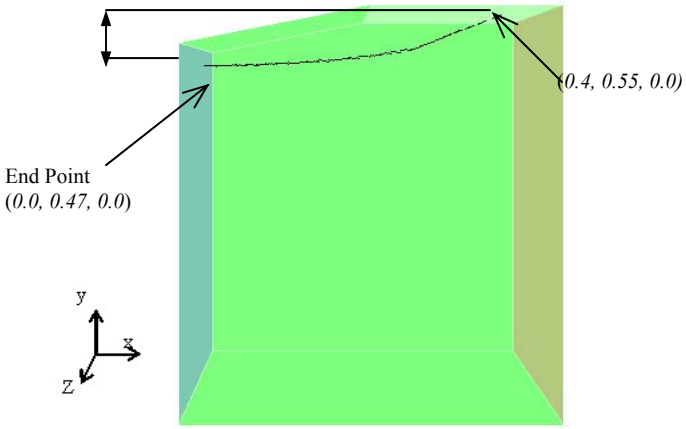

Figure 3. Fiber movement in the original design

Fiber Orientation

Figure 4 shows the movements of two PET fibers with incident angles of 20 and 30 degree. They had an initial speed of 25 m/s and field strength 250 KV/m. The modeling results show that at the end points of their trajectories, both fibers' orientations changed significantly compared to their initial incident angle. The fibers have been aligned parallel to the horizontal target direction (*x*-direction). The fiber with a 30 degree incident angle traveled longer in the vertical direction (*y*-direction). Our results also indicated that with an incident angle of 90 degrees, which means that the fiber was dropped into the alignment zone with orientation parallel to the y-axis, the fiber hit the bottom of the system before it got aligned to the field lines. In this case, the H1 and/or field strength need to be increased to provide space and/or time for the fiber to get oriented as desired.

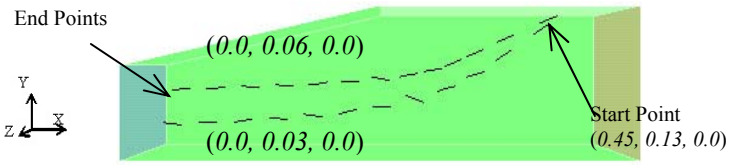

Figure 4. Change of fiber orientation in the electrostatic field

Fiber Acceleration

Generally, the electrostatic field causes the fiber to accelerate while the air drag causes the fiber to decelerate. *Figures 5–7* show the influence of different fiber types, electrostatic field strengths, and fiber diameter on speed profiles in the *x*-direction. The speed data of these figures are the average speed of the entire fiber's different segments. The negative speeds shown in *Figures 5-7* are due to the fact that fibers were dropped from $x = 0.45$ m, then moved toward $x = 0$.

The modeling results of *Figure 5* were generated for the three fibers with the same incident angle of 20 degrees, initial speed of 25 m/s, diameter of 15 microns, and field strength was 250 KV/m. Due to the fiber inertia, rayon exhibited the lowest speed decrease while nylon showed the highest speed decrease before entering the electrostatic field.

Meanwhile, it was also noticed that once the fibers entered the electrostatic field, nylon fiber gained the highest acceleration before reaching equilibrium (constant speed) since it has the smallest density. The air drag increased with square of fiber speed, but electrostatic force depends on total uni-polar charge on the fiber and field strength. All three fibers eventually reached the same equilibrium speed of 15 m/s because they had same electrical charge and diameters (the overall electrostatic force and air drag were the same).

Figure 6 shows the influence of electrostatic field strength on fiber speed profile in the *x*-direction. Modeled fibers were 15-micron PET fibers with the same incident angle of 20 degrees and initial speed of 25 m/s. For 250 kV/m field strength, the electrostatic force soon overcame air drag and accelerated the fiber until the fiber reached equilibrium. The terminal speed was 15 m/s at 250 kV/m. For 500 kV/m field strength, the electrostatic force was strong enough to continuously accelerate the fiber, and this acceleration decreased during the movement with terminal speed of 25 m/s when it hit the left electrode. While for 100 kV/m field strength, the electrostatic force can only overcome the fiber's deceleration caused by the air drag and keep the fiber moving at a constant speed of 7.3 m/s in *x*-direction. Electrostatic force is linearly proportional to the fiber charge amount and field strength, given the same charge amount. Higher field strength benefits the fiber acceleration.

Figure 7 shows the influence of fiber diameter on fiber speed. Modeled fibers were PET fibers with the same incident angle of 20 degrees and initial speed of 25 m/s; electrostatic field strength was also kept the same at 250 kV/m.

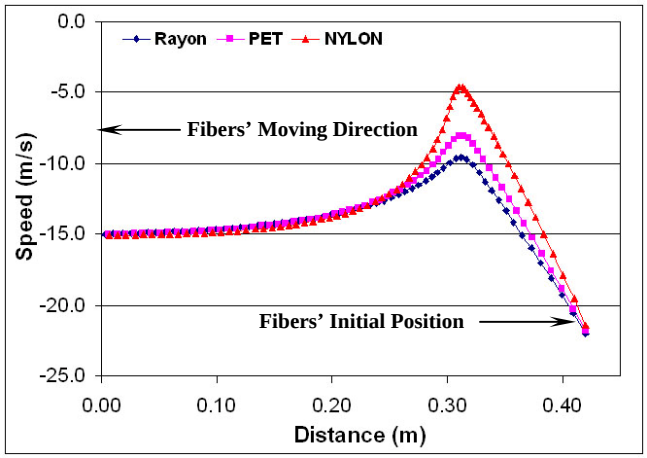

Figure 5. *x*-direction speed profiles of different types of fiber

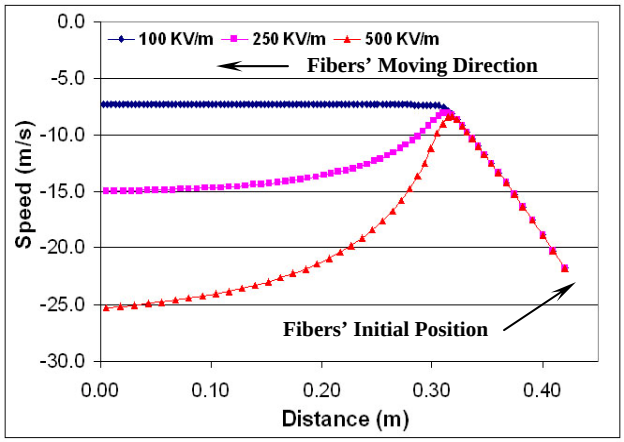

Figure 6. Influence of electrostatic field strength on fiber average speed in *x*-direction

When the fiber diameter was increased to 45 microns (approximately 20 den for PET fibers), if the total charge amount was kept the same the fiber continuously kept slowing down until it hit the electrode, since air drag increased with fiber diameter while electrostatic force was not sufficient to overcome it. But the deceleration was not as significant as that of the 15-micron fiber before entering the electrostatic field. This was because the inertia of the 45-micron fiber was much larger. When the total charge amount was increased to 12 X 10^{-11} C (this is to assume that surface charge density kept the same), the electrostatic force can reach equilibrium with the air drag to keep the fiber moving at a much higher speed (17.8 m/s).

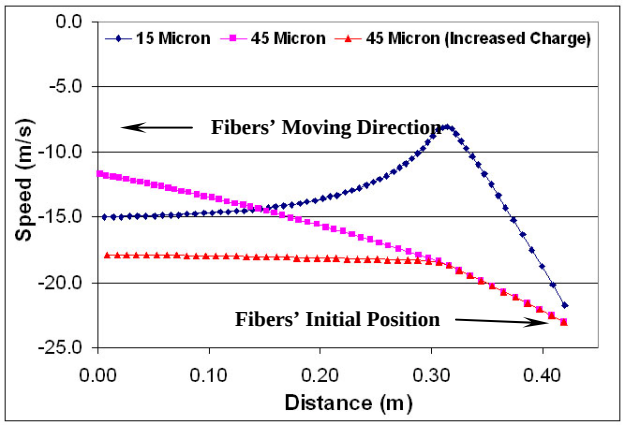

Figure 7. Influence of fiber diameter on fiber average speed in *x*-direction

CONCLUSIONS

We carried out theoretical analysis and constructed computer models for developing an innovative method that is capable of providing positive control over FOD for forming nonwoven fiberwebs. This method employs electrostatic force to achieve the control over fiber orientation. In our analysis, fiber delivery and orientation in electrostatic fields are considered in several factors, such as geometric configurations, electrostatic field, fiber type, fiber diameter and the fiber's initial conditions. Our computation shows that fibers leaving the feeding system with 20- and 30-degree incident angle can be oriented as desired in the proposed fiber orienting zone, but larger incident angle will require higher electrodes. Stronger electrostatic field strength provides higher fiber acceleration, and thus fiber will gain higher speed considering the slow-down effect caused by air drag. For fibers with lower density, air drag has more significant deceleration effect. A fiber with larger diameter experiences a higher air drag and moves at a slower speed at constant electrostatic charge.

These results can be used to optimize the equipment of the process. The findings from computer modeling can serve as a powerful tool for not only understanding how to align fibers to form fiberwebs with controlled fiber orientation using electrostatic fields, but also for obtaining nonwoven fabrics with predetermined FOD and hence engineered properties.

ACKNOWLEDGEMENT

We would like to express our sincere thanks to the National Textile Center for funding this research project.

REFERENCES

[1] Dogu,.I. "Fundamentals of Electrostatic Spinning Part I." *Textile Research Journal*, 35,521-532, 1975.

[2] Dogu,.I. "Fundamentals of Electrostatic Spinning Part II." *Textile Research Journal*, 36, 676-691, 1976.

[3] Robert, Jr., K.Q., *et al*, "New Electrostatic Spinning Concept for Cotton." *Journal of Engineering for Industry*, 106, 247-252, 1984.

[4] Yao, S.C., "Electrostatic Opening and Short Fiber Separation Apparatus for Carding Machines", US Patent 5,327,617, 1994.

[5] Ramakrishna, S., Fujihara, K., Teo, W., Lim, T.C., and Ma, Z., *An Introduction to*

Electrospinning and Nanofibers, World Scientific, 2005.

[6] Teo, W., Ramakrishna S., "A Review on Electrospinning Design and Nanofibre Assemblies", *Nanotechnology* 17, R89-R106, 2006.

[7] Theron A, Zussman E, Yarin AL, Electrostatic field-assisted alignment of electrospun nanofibers, *Nanotechnology* 12, 384-390, 2001.

[8] Nagi-Zade, A.T., and Grosberg, P. "The Manipulation of Fibers by Means of a Charged Field." *Journal of the Textile Institute*, 64, 431-436, 1973.

[9] Hou, Y. MS Thesis Fall 2001, University of Massachusetts at Dartmouth, 2001.

[10] Schlichting, H. *Boundary-layer theory*. McGraw-Hill. 1979.

AUTHORS' ADDRESS

Yiyun Cai, Ph.D.; Abdelfattah Mohamed Seyam, Ph.D.; Yong K. Kim, Ph.D.
North Carolina State University
College of Textiles
2401 Research Dr
Raleigh, NC 27695-8301
USA